

Article

DBD Plasma-ZrO₂ Catalytic Decomposition of CO₂ at Low Temperatures

Amin Zhou ¹ , Dong Chen ¹, Cunhua Ma ^{1,*}, Feng Yu ^{1,2,3}  and Bin Dai ^{1,*}

¹ School of Chemistry and Chemical Engineering, Shihezi University, Key Laboratory for Green Processing of Chemical Engineering of Xinjiang Bintuan, Shihezi 832003, China; m15699337928@163.com (A.Z.); liantian1986@sina.com (D.C.); yufeng05@mail.ipc.ac.cn (F.Y.)

² Engineering Research Center of Materials-Oriented Chemical Engineering of Xinjiang Production and Construction Corps, Shihezi 832003, China

³ Key Laboratory of Materials-Oriented Chemical Engineering of Xinjiang Uygur Autonomous Region, Shihezi 832003, China

* Correspondence: mchua@shzu.edu.cn (C.M.); dbinly@126.com (B.D.);
Tel.: +86-(0)993-2058-176 (B.D.); Fax: +86-(0)993-2057-270 (B.D.)

Received: 27 April 2018; Accepted: 14 June 2018; Published: 23 June 2018



Abstract: This study describes the decomposition of CO₂ using Dielectric Barrier Discharge (DBD) plasma technology combined with the packing materials. A self-cooling coaxial cylinder DBD reactor that packed ZrO₂ pellets or glass beads with a grain size of 1–2 mm was designed to decompose CO₂. The control of the temperature of the reactor was achieved via passing the condensate water through the shell of the DBD reactor. Key factors, for instance discharge length, packing materials, beads size and discharge power, were investigated to evaluate the efficiency of CO₂ decomposition. The results indicated that packing materials exhibited a prominent effect on CO₂ decomposition, especially in the presence of ZrO₂ pellets. Most encouragingly, a maximum decomposition rate of 49.1% (2-mm particle sizes) and 52.1% (1-mm particle sizes) was obtained with packing ZrO₂ pellets and a 32.3% (2-mm particle sizes) and a 33.5% (1-mm particle sizes) decomposing rate with packing glass beads. In the meantime, CO selectivity was up to 95%. Furthermore, the energy efficiency was increased from 3.3%–7% before and after packing ZrO₂ pellets into the DBD reactor. It was concluded that the packing ZrO₂ simultaneously increases the key values, decomposition rate and energy efficiency, by a factor of two, which makes it very promising. The improved decomposition rate and energy efficiency can be attributed mainly to the stronger electric field and electron energy and the lower reaction temperature.

Keywords: self-cooling; dielectric barrier discharge; CO₂ decomposition; CO selectivity; packing materials

1. Introduction

The fast-growing consumption of fossil fuels has resulted in continually increasing emissions of carbon dioxide, which is identified as one of the major contributors to global warming. Therefore, the decrease of environmental pollution via CO₂ emissions has attracted worldwide attention. Different strategies are being developed to address the wasted CO₂ instead of releasing it into the atmosphere, such as: carbon capture and storage, transformation and utilization of carbon and CO₂ dissociation. Direct dissociation of CO₂ into other value-added fuels and chemicals provides a potential route for efficient utilization of CO₂ and reduction of CO₂ emissions [1]. Various progresses have been explored to convert CO₂ into other value-added chemicals, such as CO₂ reforming of CH₄ for hydrogen and CO₂ hydrogenation for the synthesis of methanol, methane, formaldehyde, dimethyl, etc. [2,3]. Additionally,

direct decomposition of CO₂ into CO has also attracted great interest, which can not only relieve the pressure of economic growth, but also can achieve energy savings and emission reduction [4,5]. As a common feedstock for industry, CO is a widely-used chemical feedstock that can be used as a reactant to produce higher energy products. Not only can it be used for fuel synthesis, but also for the production of chemicals, such as organic acids, esters and other chemicals. Thus, the selective decomposition of CO₂ into CO is no doubt a promising candidate for clean energy and chemicals. However, due to the high structural stability of the CO₂ molecule, considerable energy is needed for CO₂ activation and decomposition. The conventional thermal-chemical process for CO₂ decomposition has many different levels of limited scope. For example, the thermodynamic equilibrium calculation of CO₂ conversion shows that CO₂ begins to split into CO and O₂ near 2000 K, yet with a very low conversion rate (<1%). The decomposition of CO₂ can only be carried out at an extraordinarily high temperature (3000–3500 K), which consumes high energy and involves considerable economic cost [6]. Nowadays, Non-Thermal Plasma (NTP) is a newly-developed technology, as an attractive alternative, which has been successfully applied in many fields, for instance gas purification and energy conversion [7–12]. It has advantages such as a non-equilibrium character, a low energy cost and a unique ability to initiate chemical reactions at low temperatures [13,14]. As a kind of non-thermodynamic equilibrium plasma, its distinct non-equilibrium character means the gas temperature in the plasma can be close to room temperature, whilst the electrons are highly energetic with a typical mean energy of 1–10 eV. NTP can initiate a series of chemical processes, including ionization, initiation and dissociation [15]. Various types of plasma, like glow discharge, corona discharge [16–18], microwave discharge, radio frequency discharge [19] and gliding arc discharge have been explored for CO₂ decomposition [20]. Dielectric Barrier Discharge (DBD) plasma was also tested for CO₂ splitting into CO, and it can generate high energetic electrons (1–10 eV) and initiate the chemical reactions while keeping the background temperature under ambient conditions [6]. It has been applied in many fields, such as the removal of NO_x [21], as well as the preparation of catalysts [22] and other materials [23]. The decomposition and conversion of the stable CO₂ using DBD plasma is no exception, which has attracted increasing attention for its unique abilities.

Many relevant works have been reported for the direct decomposition of pure CO₂, CO₂ conversion or reacting with other gases, such as adding inert gases to dilute the pure CO₂ under the assistance of DBD plasma [24,25]. It was reported that nitrogen is more effective for CO₂ decomposition among argon, nitrogen and helium as diluents, but this will produce unwanted by-products inevitably, which is not preferable from the industrial application point of view [26]. Therefore, many previous works have focused on the dissociation or conversion of CO₂ without diluting. Further fundamental works reported that different packing dielectric materials can enhance the conversion of CO₂ and improve the energy efficiency of the plasma process [14]. Yu et al. investigated the conversion of CO₂ in a packed-bed DBD reactor using silica gel, quartz, α -Al₂O₃, γ -Al₂O₃ and CaTiO₃ as packing materials and proved that the introduction of dielectric materials into the plasma reactor resulted in an increased electric field, which then increased the electron energy and led to an expected higher CO₂ conversion [27]. Similarly, a series of Ca_xSr_(1-x)TiO₃ has also been used as a dielectric material for the splitting of CO₂ in a DBD reactor to prove the importance of the high permittivity dielectrics, which can increase the discharge power of plasma accompanied by dense and strong micro-discharges, thereby significantly enhancing the decomposition of CO₂ [28–30]. Yap et al. [31] reported the best conversion with an Alternating Current (AC) sinusoidal activation when using the glass beads as packing materials. In recent reports, CeO₂ was packed to understand the oxygen storage/release capacity on the improvement of CO₂ conversion in the packed DBD reactor [32]. Duan et al. [33] obtained a CO₂ conversion of 41.9% in a CaO-packed DBD micro-plasma reactor. Mei et al. [34] proved that in the coaxial dielectric barrier discharge reactor, the discharge power was the most important factor that affected the CO₂ conversion. Furthermore, they showed that BaTiO₃ pellets exhibited a better performance than TiO₂ pellets and glass beads due to the higher dielectric constant and the better

synergistic effect of plasma-catalysis [6,34]. Moreover, the design of the reactor is also of importance for CO₂ conversion [35].

In this study, a self-cooling coaxial cylinder DBD reactor was applied to decompose pure CO₂ into CO and O₂ at atmospheric pressure and ambient temperature, which was the same as the previous apparatus of Zhou et al. [36]. The commercial ZrO₂ pellets and glass beads were used as packing materials to demonstrate the improvement of the decomposition rate and energy efficiency for CO₂ splitting. Condensate water can take away the heat that is introduced in the process of plasma discharge to maintain the temperature of the reactor. Key factors like packing materials and discharge power, discharge length and bead size were investigated to evaluate the efficiency of CO₂ decomposition. Interestingly, a high decomposition rate and energy efficiency could be obtained. The physical discharge characteristics of DBD plasma were also investigated to understand the interactions between the dielectric materials and DBD plasma in CO₂ decomposition.

2. Results and Discussion

2.1. Effect of Discharge Length on CO₂ Decomposition Rate and Energy Efficiency

In order to further be sure of the influence of DBD plasma on the decomposition of CO₂, the discharge length of the unpacked DBD reactor was changed to conduct the experiment. As Figure 1a shows, the CO₂ decomposition rate increased clearly with the increasing discharge length. This can be attributed to competing effects primarily. Firstly, increasing the discharge length from 100–200 mm significantly increased the residence time of CO₂ gas in the reactor, which positively increased the probability of CO₂ molecules colliding with highly energetic electrons and reactive species [34]. However, a longer discharge region will need increasing surface area of the DBD reactor, leading to higher energy loss due to heat dissipation [37], as shown in Figure 1b. In this study, increasing the discharge length significantly increased the residence time of CO₂ in the reaction, which plays a more dominant role in the decomposition of CO₂ compared to the negative effects (e.g., increased energy loss); therefore, 200 mm was chosen as the optimum discharge length to conduct the experiment.

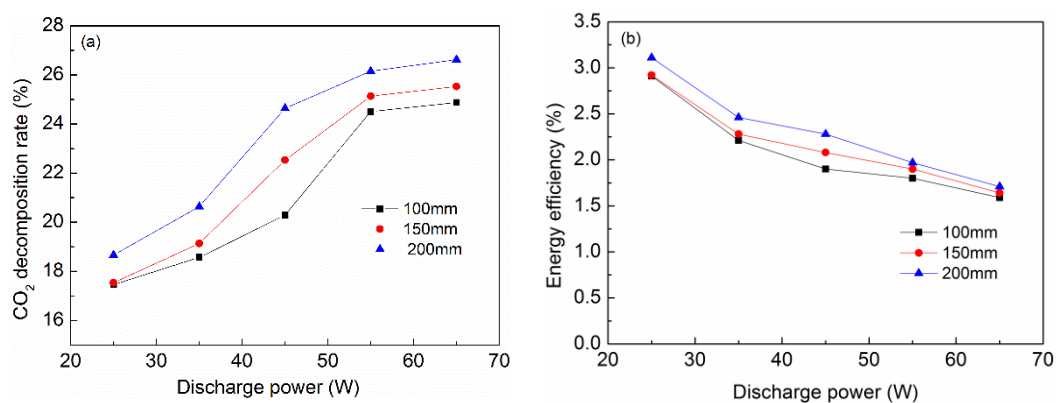


Figure 1. CO₂ decomposition rate (a) and energy efficiency (b) in the reactor without packing at different discharge powers (frequency: 12 kHz; feed flow rate: 20 mL/min; 20 °C condensate water).

2.2. Effect of Discharge Power and Beads Size on CO₂ Decomposition and Energy Efficiency

The CO₂ decomposition rate as a function of bead size at different discharge powers is illustrated in Figure 2. ZrO₂ and glass beads with a size of 1 mm and 2 mm were applied to investigate the influence on CO₂ decomposition. Figure 2a shows that the smaller bead size was more beneficial for CO₂ decomposition under other fixed conditions. When decreasing the beads size, more dielectric spheres would be needed to fill the reactor, which increased the discharge surface area, reinforced the surface discharge and hence, caused, a higher CO₂ decomposition rate. Similarly, Van Laer and

Bogaerts [38] reported that a suitable range of bead size was needed to obtain a high CO₂ decomposition and energy efficiency.

Discharge power is also one of the key factors influencing CO₂ decomposition in the DBD plasma technique. According to associated reports, the discharge power determined whether there was sufficient energy for activating and decomposing the CO₂ molecule [6]. The CO₂ decomposition rate and energy efficiency at different discharge powers in the DBD reactor are shown in Figure 2a,b. There is a general observation that the CO₂ degradation rate increased with the increasing discharge power, but the energy efficiency was affected in the opposite manner. A higher discharge power meant more energy was injected into this system, therefore generating more chemically-active species and reactant molecules in the reaction, and enough energy would activate electron and reactant molecules, as well as increase the mutual collision opportunities between active species, so more chemical bonds would be broken and more active substances formed. However, the CO₂ decomposition rate tends to saturate when the discharge power rises above 55 W, so a suitable range of discharge power is necessary from the viewpoint of energy savings. Furthermore, the reason for the decreased energy efficiency with the increasing discharge power could be due to the lost energy, which was consumed as heat, and it can be evidenced by the increasing temperature of the condensate water. At the same discharge power of 55 W, the CO₂ decomposition rate in the unpacked reactor was 26.1%, but it reached 33.5% and 52.1% when the DBD reactor was packed with 1-mm glass beads and ZrO₂ pellets, respectively. Meanwhile, the energy efficiency only in ZrO₂ pellets packing was also improved by a factor of two.

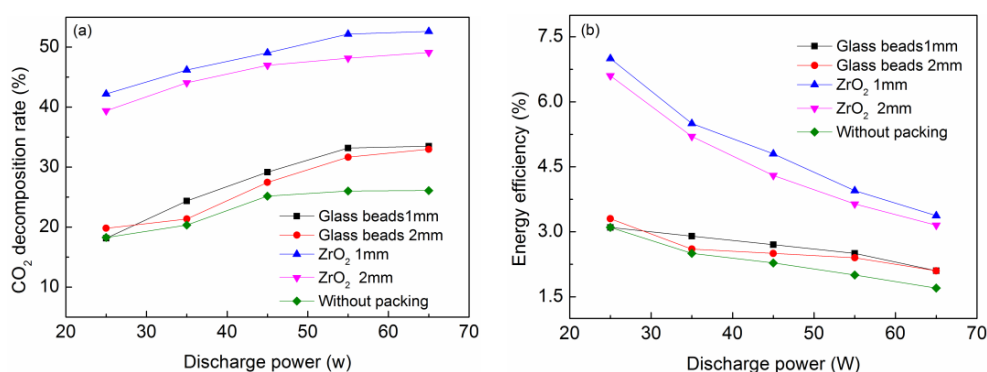


Figure 2. CO₂ decomposition rate (a) and energy efficiency (b) using different packing bead sizes at different discharge powers (frequency: 12 kHz; feed flow rate: 20 mL/min; 20 °C condensate water; discharge length: 200 mm).

Three reasons may account for this result. Firstly, filling materials in the discharge zone made a more stable, uniform and stronger discharge, and all these were favorable for higher CO₂ decomposition because it meant more CO₂ molecules were activated. Additionally, the intensity of the electric field between the contact points of the pellets to pellets or the pellets to the reactor wall could be enhanced because of the polarization of the dielectric materials. Though the electric field was enhanced by the increased discharge power regardless of the packing materials used [27], the presence of packing materials may have further strengthened the average electric field near contact points of the pellets, heightening the electric electron temperature, which facilitated electron collision [39,40], hence causing a higher CO₂ decomposition rate in the packed reactor. The morphology of ZrO₂ pellets may also be conducive to the transfer of electrons, thus accelerating the decomposition of CO₂. Because ZrO₂ is a kind of high performance structure ceramic material, it owns a higher dielectric constant (27) than glass beads (9), which is proven to play a significant role in CO₂ decomposition [39]. In addition, ZrO₂ is also a kind of basic oxide, and it plays an important role in CO₂ decomposition due to the acidity of CO₂. This was proved in Duan X's study: the base properties of the packing materials affected the chemisorption of CO₂ in the process of CO₂ decomposition [34]. That is advantageous to CO₂ decomposition.

Furthermore, ZrO_2 exhibits better reaction activity than glass beads possibly due to the fast oxygen ion migration rate of ZrO_2 [41,42], so the oxygen containing active substances was produced on the surface of ZrO_2 pellets, or oxygen ions could be quickly transferred, thus inhibiting the recombination of oxygen free radicals with the generated CO to promote the continuous decomposition of CO_2 . In addition, the thermal conductivity of ZrO_2 is higher than that of glass. It may also contribute to the energy transfer in the reaction process and the activation of CO_2 molecules. Therefore, ZrO_2 enhanced the CO_2 decomposition compared to glass beads.

2.3. Effect of Packing Materials on Discharge Characteristics

It can be noticed from the V-Q curve of the CO_2 discharge that the characteristics vary in the reactor with and without packing. A typical filamentary discharge in the discharge with no packing can be observed, and this be confirmed by the numerous peaks in the discharge signal of Figure 3a. In contrast, as is shown in Figure 3b,c, packing ZrO_2 or glass beads into the discharge zone generates a typical packed-bed effect and leads to a transition in the discharge behavior from a filamentary discharge to a combination of surface discharge and filamentary discharge, because of the decrease of the spikes in the discharge signal.

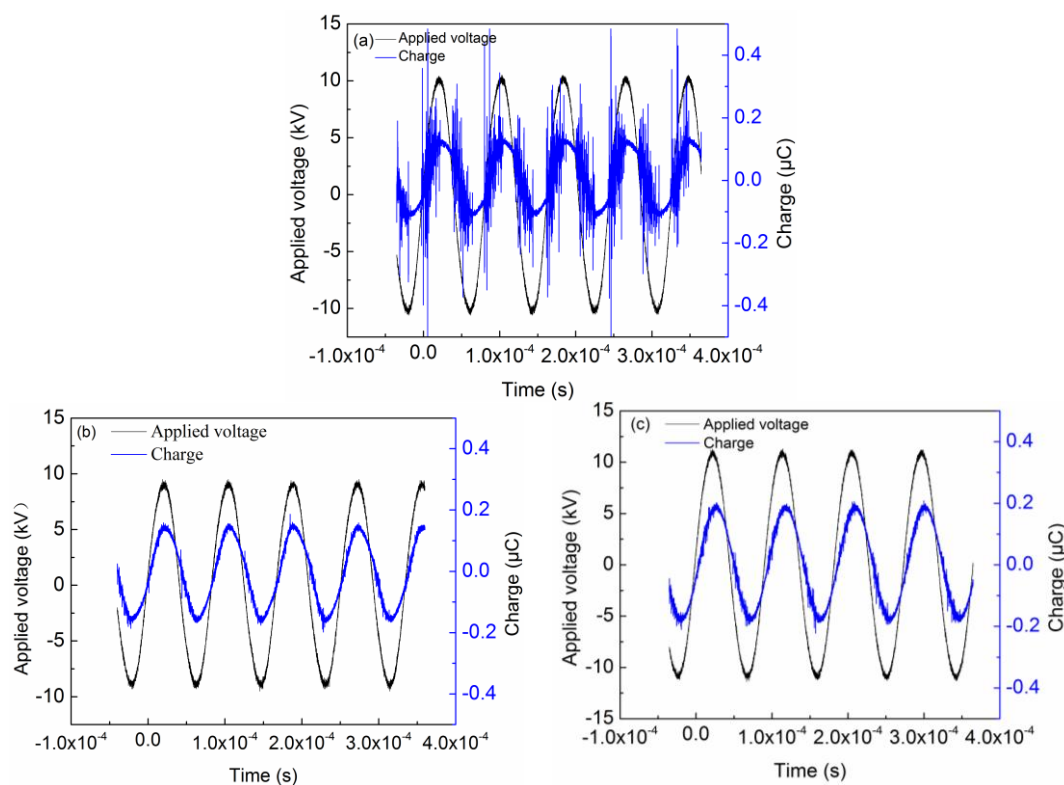


Figure 3. Discharge characteristics of CO_2 in the Dielectric Barrier Discharge (DBD) reactor with or without packing: (a) without packing; (b) glass beads; (c) ZrO_2 (discharge power: 55 W; feed flow rate: 20 mL/min; 20 °C condensate water; discharge length: 200 mm; beads size: 1 mm).

Figure 4 presents the Lissajous figure of CO_2 decomposition in the DBD reactor with or without packing materials, at the discharge power of 55 W. It shows the change of the discharge characteristic during the decomposition of CO_2 . Compared with non-packing materials, the Lissajous figure changed from a parallelogram to an oval shape when ZrO_2 pellets or glass beads were filled in the DBD reactor. At the same discharge power, the applied voltage increased from 9.8 kV (pk-pk) without packing to 11.5 kV with the ZrO_2 packing and to 10.6 kV (pk-pk) with the glass bead packing. It was obviously observed that the discharge mode varied from filamentary discharge to a mode of filamentary discharge

combined with surface discharge, and we could obtain a more stable and uniform discharge form. As a result, the introduction of packing materials into the DBD reactor had a promotional effect on the discharge characteristics. Yu et al. [27] also published a consistent report on the discharge characteristics of CO₂ conversion in the dielectric packed-bed plasma reactor, and the result was further proved by Mei et al. [6]. The introduction of packing materials caused the presence of a strong electrical field and thus led to a high electron energy near the contact points of the pellets, hence the improved CO₂ decomposition.

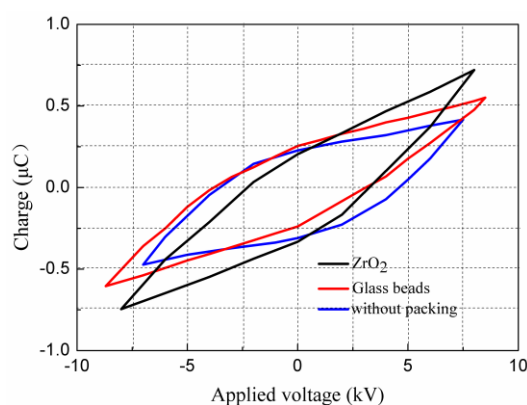


Figure 4. Lissajous figure of CO₂ decomposition in the DBD reactor with or without packing materials (discharge power: 55 W; feed flow rate: 20 mL/min; 20 °C condensate water; discharge length: 200 mm; beads size: 1 mm).

2.4. Effect of Packing Materials on CO Selectivity

The function of discharge power on CO selectivity is presented in the Figure 5a. The selectivity of CO throughout the reaction remained around 94–96%, and the difference of CO selectivity in different discharge power was not obvious in our experimental condition. It can be concluded that discharge power played a minor role in the CO selectivity. The CO₂ decomposition at the same discharge power and feed flow rate was also conducted to investigate the effect of packing materials on CO selectivity, as is shown in Figure 5b. The CO selectivities of the three different conditions were almost the same, and the CO selectivity remained at about 95% regardless of the packing materials. It can be concluded that packing materials played a minor role in the CO selectivity using self-cooling dielectric barrier discharge plasma.

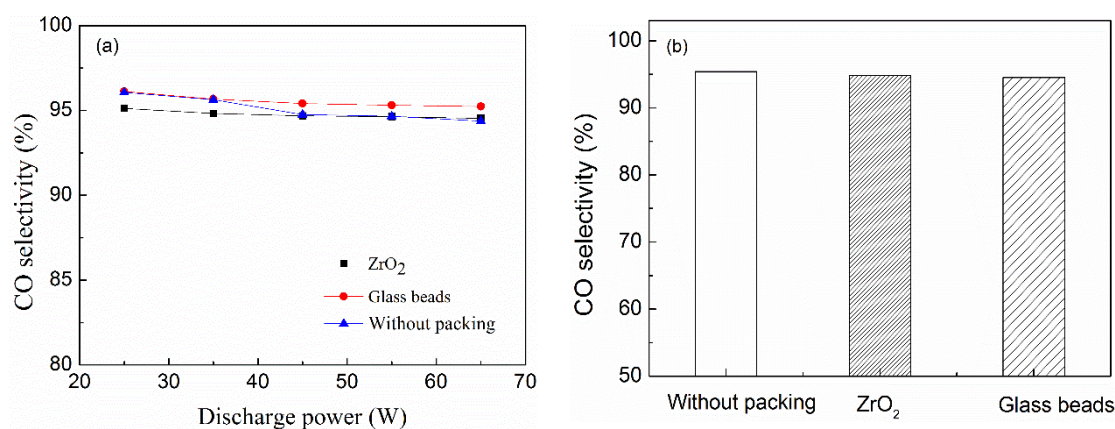


Figure 5. (a) CO selectivity at different discharge powers; (b) CO selectivity at a discharge power of 55 W (frequency: 12 kHz; feed flow rate: 20 mL/min; 20 °C condensate water; discharge length: 200 mm; bead size: 1 mm).

2.5. The Investigation of Carbon Deposition

After reaction, some black carbon deposition was clearly observed on the surface of the inner electrode and ZrO_2 pellets present in the discharge zone, suggesting that carbon was produced during the CO_2 decomposition in the DBD plasma combined with ZrO_2 . Figure 6 is the SEM pictures of the surface of ZrO_2 pellets before and after the reaction; it shows that the surface of the ZrO_2 pellets was covered with carbon deposition. Because high energy electrons generated by the DBD plasma had a range of 1–10 eV [35], which was not enough for the dissociation of CO molecules, because of its high dissociation energy (11 eV), the carbon deposition may have come from the decomposition of CO_2 at temperatures higher than 20 °C of condensate water.

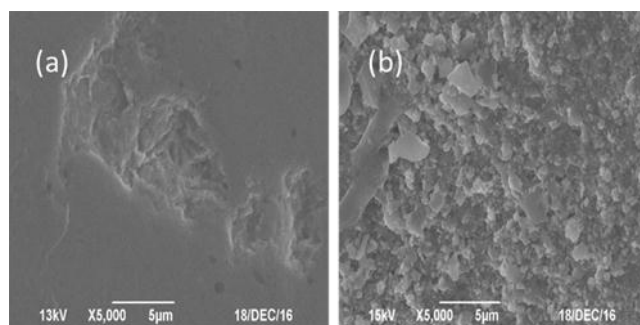


Figure 6. SEM images of carbon deposition on the surface of ZrO_2 pellets (a) before the reaction and (b) after the reaction.

2.6. Reaction of CO and O_2

To gain insight into the role of packing dielectric materials and the principles of the CO_2 decomposition, the oxidation of CO, which is the reverse reaction of CO_2 decomposition, was still investigated using ZrO_2 pellets and glass beads as the packing materials at different discharge powers, and the results are shown in Figure 7. CO conversion increased with the increasing discharge power. Apparently, the CO conversion without packing was higher than that of the packed DBD reactor. Though ZrO_2 exhibited a promotional effect on the CO_2 decomposition, it was not conducive for CO conversion at the same condition. In all cases, CO_2 was formed as the only product, and no carbon deposition was generated. This was in agreement with the above result that CO could not split into C in this condition due to its high dissociation energy of CO molecules (11.1 eV). Therefore, the DBD plasma conditions with electron energy in the range of 1–10 eV were optimum for the electron impact dissociation of CO_2 [27].

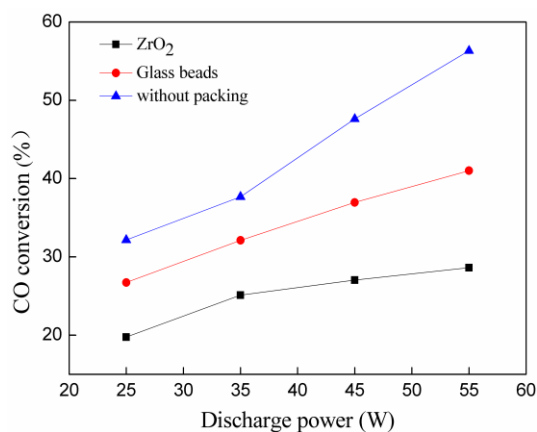


Figure 7. CO oxidation at different discharge powers (frequency: 12 kHz; feed flow rate: 20 mL/min; 20 °C condensate water; beads size: 1 mm).

2.7. Comparison of Obtained Values in Different Packed DBD Reactors

Table 1 shows the compared values of the CO₂ decomposition and energy efficiency using different packed DBD reactors. Though the DBD reactor made of quartz has been widely applied for CO₂ decomposition, the self-cooling DBD reactor made of Pyrex glass can also be utilized for CO₂ decomposition [37]. A relatively higher CO₂ decomposition rate, together with a stable CO selectivity, was obtained when using the same packing materials like ZrO₂ pellets. Fifty two-point-one percent (1-mm ZrO₂) of the CO₂ decomposition rate was an accurate value, which has been repeatedly verified.

Table 1. Obtained values in different packed DBD plasma reactors.

Packing Materials	ZrO ₂	ZrO ₂	BaTiO ₃	BaTiO ₃	CaTiO ₃
Reactor	Quartz	Glass	Quartz	Quartz	Quartz
Decomposition rate (%)	42	52.1	28	38.3	20.5
Energy efficiency (%)	9.6	7.0	7.1	17	4.8
CO selectivity (%)	50	94–96	—	—	—
Power (w)	60	55	50	—	35.3
Reference	38	This work	6	35	27

3. Experimental Setup

Figure 8 shows the schematic diagram of the experimental setup, which is basically consistent with the previous apparatus in Zhou et al. [37]. It contains 3 parts: a DBD plasma reactor, a flow control device and a GC detection and analysis system. The experiments were performed using a self-cooling DBD reactor (BEIJING SYNTHWARE GLASS, Beijing, China) made of Pyrex, which consisted of a double coaxial cylinder, a High-Voltage (HV) electrode and a Low-Voltage (LV) electrode. The HV electrode was a stainless steel rod (2 mm in diameter), on which a 1 mm-thick copper wire was wrapped, and it was installed in the axis of the double coaxial glass cylinder and linked to an alternating current power supply. Condensate water used as a cooling agent was fed into the shell of the concentric cylinder DBD reactor. The LV electrode that grounded by a wire placed into condensate water. The HV and LV electrodes formed a cylindrical discharge space.

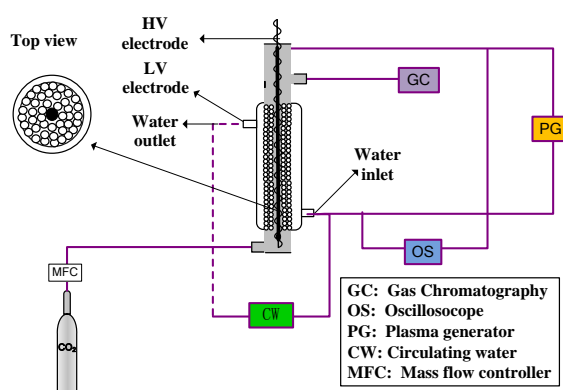


Figure 8. The schematic of the experimental setup.

During the course of the experiment, condensate water can take away the heat produced during plasma discharge, to keep the temperature of the reactor at the designed temperature. It has been proven that decreasing the temperature of the reactor was advantageous to CO₂ decomposition [43,44]. In this work, we controlled the temperature of the condensed water at 20 °C, while this value was optimized in Zhou et al. [37]. The flow rate of pure CO₂ was fixed at 20 mL/min. The applied voltage was measured by a high-voltage probe (Tektronix P6015A), and the current was recorded by a current monitor. The voltage on the external capacitor was measured to obtain the charge generated in the

discharge. All of the electrical signals were sampled by a four-channel digital oscilloscope (TDS3054B). The discharge power was obtained by the area calculation of the Q - U Lissajous figure. The gas products were analyzed by gas chromatography (GC-2014C), which was equipped with a thermal conductivity detector (TCD), and H_2 was used as the carrier gas. For comparison, CO_2 decomposition was also carried out in the DBD reactor without packing materials.

In this study, ZrO_2 pellets and glass beads with a grain size of 1–2 mm were fully packed in the discharge area as dielectric packing materials, both of which were commercial reagents without any treatment (Shanghai Gongtao Ceramics Co., Ltd., Shanghai, China).

To evaluate the performance of the plasma process, the Specific Input Energy (SIE), CO_2 decomposing rate and selectivity towards CO were defined as follows:

$$CO_2 \text{ decomposition rate (\%)} = \frac{CO_2 \text{ decomposed}}{CO_2 \text{ input}} \times 100\%$$

$$CO \text{ selectivity (\%)} = \frac{CO \text{ formed}}{CO_2 \text{ decomposed}} \times 100\%$$

$$\text{Energy efficiency } (\eta) = \frac{\Delta H \times CO_2 \text{ decomposed} \times F}{60 \times V_m \times P} \times 100\%$$

where P is the discharge power, F is the feed flow rate (mL/min) of CO_2 , ΔH is the enthalpy of reaction: $CO_2 \rightarrow CO + \frac{1}{2}O_2$, $\Delta H = 279.8$ kJ/mol and $V_m = 22.4$ L/mol, and V_m is the molar volume.

4. Conclusions

Decomposition of CO_2 into CO and O_2 has been carried out in a self-cooling DBD plasma reactor packed with ZrO_2 and glass beads at low temperatures and ambient pressure. It could be concluded that a longer discharge length and a smaller bead size were beneficial for CO_2 decomposition. The introduction of packing materials shifted the discharge mode from filamentary discharge to a combination of filamentary and surface discharge. In comparison with the CO_2 decomposition rate in the empty reactor and glass-packed reactor, which reached 26.1% and 33.5%, respectively, a CO_2 decomposition rate of 52.1% was obtained in the ZrO_2 (1 mm) packed DBD reactor at the same condition. ZrO_2 exhibited a superior promotional effect on the decomposition of CO_2 and energy efficiency by up to a factor of 1.9 and 2.1, respectively, compared with the result of the unpacked DBD reactor. Additionally, the main product of this work was CO, with slight carbon deposition that came from the dissociation of CO_2 . The results indicated that the dielectric constant and particle morphology of the packing materials matter greatly in the decomposition of CO_2 .

Author Contributions: A.Z. and B.D. designed and administered the experiments. A.Z. and B.D. performed the experiments. A.Z., D.C., C.M. and F.Y. collected and analyzed the data. All authors discussed the data and wrote the manuscript.

Acknowledgments: This work was financially supported by the National Natural Science Foundation of China (No. 21663022) and the High-level Talent Scientific Research Project in Shihezi University (No. RCZX201406).

Conflicts of Interest: The authors declare no conflict of interest.

References

1. Razali, N.; Lee, K.T.; Bhatia, S.; Mohamed, A.R. Heterogeneous catalysts for production of chemicals using carbon dioxide as raw material: A review. *Renew. Sustain. Energy Rev.* **2012**, *16*, 4951–4964. [[CrossRef](#)]
2. Centi, G.; Quadrelli, E.A.; Perathoner, S. Catalysis for CO_2 conversion: A key technology for rapid introduction of renewable energy in the value chain of chemical industries. *Energy Environ. Sci.* **2013**, *6*, 1711–1731. [[CrossRef](#)]
3. Lebouvier, A.; Iwarere, S.A.; Argenlieu, P.D.; Ramjugernath, D.; Fulcheri, L. Assessment of carbon dioxide dissociation as a new route for syngas production: A Comparative review and potential of plasma-Based technologies. *Energy Fuels* **2013**, *27*, 2712–2722. [[CrossRef](#)]

4. Ayzner, A.L.; Wanger, D.D.; Tassone, C.J.; Tolbert, S.H.; Schwartz, B.J. Room to improve conjugated polymer-based solar cells: Understanding how thermal annealing affects the fullerene component of a bulk heterojunction photovoltaic device. *J. Phys. Chem. C* **2008**, *112*, 18711–18716. [[CrossRef](#)]
5. Kim, S.S.; Sang, M.L.; Hong, S.C. A study on the reaction characteristics of CO₂ decomposition using iron oxides. *J. Ind. Eng. Chem.* **2012**, *18*, 860–864. [[CrossRef](#)]
6. Mei, D.; Zhu, X.; He, Y.L.; Yan, J.D.; Tu, X. Plasma-assisted conversion of CO₂ in a dielectric barrier discharge reactor: Understanding the effect of packing materials. *Plasma Sour. Sci. Technol.* **2015**, *24*, 015011. [[CrossRef](#)]
7. Aerts, R.; Tu, X.; De Bie, C.; Whitehead, J.C.; Bogaerts, A. An Investigation into the dominant reactions for ethylene destruction in non-thermal atmospheric plasmas. *Plasma Process. Polym.* **2012**, *9*, 994–1000. [[CrossRef](#)]
8. Harling, A.M.; Glover, D.J.; Whitehead, J.C.; Zhang, K. Novel method for enhancing the destruction of environmental pollutants by the combination of multiple plasma discharges. *Environ. Sci. Technol.* **2008**, *42*, 4546–4550. [[CrossRef](#)] [[PubMed](#)]
9. Liu, S.; Mei, D.; Shen, Z.; Tu, X. Non-oxidative conversion of methane in a dielectric barrier discharge reactor: Prediction of reaction performance based on neural model. *J. Phys. Chem. C* **2014**, *118*, 10686–10693. [[CrossRef](#)]
10. Snoeckx, R.; Aerts, R.; Tu, X.; Bogaerts, A. Plasma-based dry reforming: A computational study ranging from nanoseconds to seconds timescale. *J. Phys. Chem. A* **2013**, *117*, 4857–4970. [[CrossRef](#)]
11. Xin, T.; Whitehead, J.C. Plasma dry reforming of methane in an atmospheric pressure AC gliding arc discharge: Co-generation of Syngas and carbon nanomaterials. *Int. J. Hydrog. Energy* **2014**, *39*, 9658–9669.
12. Yu, L.; Tu, X.; Li, X.; Wang, Y.; Chi, Y.; Yan, J. Destruction of acenaphthene, fluorene, anthracene and pyrene by a dc gliding arc plasma reactor. *J. Hazard. Mater.* **2010**, *180*, 449–455. [[CrossRef](#)] [[PubMed](#)]
13. Tu, X.; Gallon, H.J.; Twigg, M.V.; Gorry, P.A.; Whitehead, J.C. Dry reforming of methane over a Ni/Al₂O₃ catalyst in a coaxial dielectric barrier discharge reactor. *J. Phys. D Appl. Phys.* **2011**, *44*, 274007. [[CrossRef](#)]
14. Tu, X.; Whitehead, J.C. Plasma-catalytic dry reforming of methane in an atmospheric dielectric barrier discharge: Understanding the synergistic effect at low temperature. *Appl. Catal. B Environ.* **2012**, *125*, 439–448. [[CrossRef](#)]
15. Wang, B.; Yan, W.; Ge, W.; Duan, X. Kinetic model of the methane conversion into higher hydrocarbons with a dielectric barrier discharge microplasma reactor. *Chem. Eng. J.* **2013**, *234*, 354–360. [[CrossRef](#)]
16. Horvath, G.; Skalny, J.D.; Mason, N.J. FTIR study of decomposition of carbon dioxide in DC corona discharges. *J. Phys. D Appl. Phys.* **2008**, *41*, 207–225. [[CrossRef](#)]
17. Mikoviny, T.; Kocan, M.; Matejcek, S.; Mason, N.J.; Skalny, J.D. Experimental study of negative corona discharge in pure carbon dioxide and its mixtures with oxygen. *J. Phys. D Appl. Phys.* **2003**, *37*, 64–73. [[CrossRef](#)]
18. Wen, Y.; Jiang, X. Decomposition of CO₂ Using Pulsed Corona Discharges Combined with Catalyst. *Plasma Chem. Plasma Process.* **2001**, *21*, 665–678. [[CrossRef](#)]
19. Kozak, T.; Bogaerts, A. Splitting of CO₂ by vibrational excitation in non-equilibrium plasmas: A reaction kinetics model. *Plasma Sour. Sci. Technol.* **2014**, *23*, 045004. [[CrossRef](#)]
20. Nunnally, T.; Gustol, K.; Rabinovich, A.; Fridman, A.; Gutsol, A.; Kemoun, A. Dissociation of CO₂ conversion in a low current gliding arc plasmatron. *J. Phys. D Appl. Phys.* **2011**, *44*, 274009. [[CrossRef](#)]
21. Zhao, D.; Yu, F.; Zhou, A.; Ma, C.; Dai, B. High-efficiency removal of NO_x using dielectric barrier discharge nonthermal plasma with water as an outer electrode. *Plasma Sci. Technol.* **2018**, *20*, 014020. [[CrossRef](#)]
22. Zhang, M.; Li, P.; Zhu, M.; Tian, Z.; Dan, J.; Li, J.; Wang, Q. Ultralow-weight loading Ni catalyst supported on two-dimensional vermiculite for carbon monoxide methanation. *Chin. J. Chem. Eng.* **2017**. [[CrossRef](#)]
23. Wang, Y.; Yu, F.; Zhu, M.; Ma, C.; Zhao, D.; Wang, C.; Zhou, A.; Guo, X. N-doping of plasma exfoliated graphene oxide via dielectric barrier discharge plasma treatment for oxygen reduction reaction. *J. Mater. Chem. A* **2018**, *6*, 2011–2017. [[CrossRef](#)]
24. Indarto, A.; Yang, D.R.; Choi, J.W.; Lee, H.; Song, H.K. Gliding arc plasma processing of CO₂ conversion. *J. Hazard. Mater.* **2007**, *146*, 309–315. [[CrossRef](#)] [[PubMed](#)]
25. Nozaki, T.; Okazaki, K. Non-thermal plasma catalysis of methane: Principles, energy efficiency, and applications. *Catal. Today* **2013**, *211*, 29–38. [[CrossRef](#)]

26. Ozkan, A.; Dufour, T.; Arnoult, G.; Keyzer, P.D.; Bogaerts, A.; Reniers, F. CO₂-CH₄ conversion and syngas formation at atmospheric pressure using a multi-electrode dielectric barrier discharge. *J. CO₂ Util.* **2015**, *9*, 74–81. [[CrossRef](#)]
27. Yu, Q.; Kong, M.; Liu, T.; Fei, J.; Zheng, X. Characteristics of the Decomposition of CO₂ in a Dielectric Packed-Bed Plasma Reactor. *Plasma Chem. Plasma Process.* **2012**, *32*, 153–163. [[CrossRef](#)]
28. Li, R.; Tang, Q.; Shu, Y.; Sato, T. Investigation of dielectric barrier discharge dependence on permittivity of barrier materials. *Appl. Phys. Lett.* **2007**, *90*, 131502. [[CrossRef](#)]
29. Li, R.; Tang, Q.; Yin, S.; Yamaguchi, Y.; Sato, T. Decomposition of carbon dioxide by the dielectric barrier discharge (DBD) Plasma Using Ca_{0.7}Sr_{0.3}TiO₃ barrier. *Chem. Lett.* **2004**, *33*, 412–413. [[CrossRef](#)]
30. Wang, S.; Zhang, Y.; Liu, X.; Wang, X. Enhancement of CO₂ conversion rate and conversion efficiency by homogeneous discharges. *Plasma Chem. Plasma Process.* **2012**, *32*, 979–989. [[CrossRef](#)]
31. Yap, D.; Tatibouet, J.M.; Batiot-Dupeyrat, C. Carbon dioxide dissociation to carbon monoxide by non-thermal plasma. *J. CO₂ Util.* **2015**, *12*, 54–61. [[CrossRef](#)]
32. Ray, D.; Subrahmanyam, C. CO₂ decomposition in a packed dbd plasma reactor: Influence of packing materials. *RSC Adv.* **2016**, *6*, 39492–39499. [[CrossRef](#)]
33. Duan, X.; Hu, Z.; Li, Y.; Wang, B. Effect of dielectric packing materials on the decomposition of carbon dioxide using dbd microplasma reactor. *AIChE J.* **2015**, *61*, 898–903. [[CrossRef](#)]
34. Mei, D.; He, Y.; Liu, S.; Yan, J.; Tu, X. Optimization of CO₂ conversion in a cylindrical dielectric barrier discharge reactor using design of experiments. *Plasma Process. Polym.* **2016**, *13*, 544–556. [[CrossRef](#)]
35. Mei, D.; Zhu, X.; Wu, C.; Ashford, B.; Williams, P.T.; Tu, X. Plasma-photocatalytic conversion of CO₂ at low temperatures: Understanding the synergistic effect of plasma-catalysis. *Appl. Catal. B Environ.* **2016**, *182*, 525–532. [[CrossRef](#)]
36. Mei, D.; Tu, X. Conversion of CO₂ in a cylindrical dielectric barrier discharge reactor: Effects of plasma processing parameters and reactor design. *J. CO₂ Util.* **2017**, *19*, 68–78. [[CrossRef](#)]
37. Zhou, A.; Chen, D.; Dai, B.; Ma, C.; Li, P.; Yu, F. Direct decomposition of CO₂ using self-cooling dielectric barrier discharge plasma. *Greenh. Gases Sci. Technol.* **2017**, *7*, 721–730. [[CrossRef](#)]
38. Van Laer, K.; Bogaerts, A. Improving the conversion and energy efficiency of carbon dioxide splitting in a zirconia-packed dielectric barrier discharge reactor. *Energy Technol.* **2015**, *3*, 1038–1044. [[CrossRef](#)]
39. Ozkan, A.; Dufour, T.; Silva, T.; Britun, N.; Snyders, R.; Bogaerts, A.; Reniers, F. The influence of power and frequency on the filamentary behavior of a flowing DBD-application to the splitting of CO₂. *Plasma Sour. Sci. Technol.* **2016**, *25*, 025013. [[CrossRef](#)]
40. Dou, B.; Feng, B.; Wang, C.; Jia, Q.; Li, J. Discharge characteristics and abatement of volatile organic compounds using plasma reactor packed with ceramic Raschig rings. *J. Electrostat.* **2013**, *71*, 939–944. [[CrossRef](#)]
41. Jiang, Q.; Chen, Z.; Tong, J.; Yang, M.; Jiang, Z.; Li, C. Direct thermolysis of CO₂ into CO and O₂. *Chem. Commun.* **2017**, *53*, 1188–1191. [[CrossRef](#)] [[PubMed](#)]
42. Mahato, N.; Banerjee, A.; Gupta, A.; Omar, S.; Balani, K. Progress in material selection for solid oxide fuel cell technology: A review. *Prog. Mater. Sci.* **2015**, *72*, 141–337. [[CrossRef](#)]
43. Zhang, K.; Zhang, G.; Liu, X.; Phan, A.N.; Luo, K. A study on CO₂ decomposition to CO and O₂ by the combination of catalysis and dielectric barrier discharges at low temperatures and ambient pressure. *Ind. Eng. Chem. Res.* **2017**, *56*, 3204–3216. [[CrossRef](#)]
44. Ozkan, A.; Bogaerts, A.; Reniers, F. Routes to increase the conversion and the energy efficiency in the splitting of CO₂ by a dielectric barrier discharge. *J. Phys. D Appl. Phys.* **2017**, *50*, 084004. [[CrossRef](#)]

